The Journal of Experimental Biology 203, 3425–3434 (2000)
Printed in Great Britain © The Company of Biologists Limited 2000
JEB2771

THE MEMBRANE PERMEABILITY TRANSITION IN LIVER MITOCHONDRIA OF THE GREAT GREEN GOBY *ZOSTERISESSOR OPHIOCEPHALUS* (PALLAS)

A. TONINELLO[1,*], M. SALVI[1] AND L. COLOMBO[2]

[1]*Dipartimento di Chimica Biologica dell'Università di Padova, Centro delle Biomembrane del C.N.R., Italy* and [2]*Dipartimento di Biologia dell'Università di Padova, Viale G. Colombo 3, 35121 Padova, Italy*

*e-mail: toninell@bio.civ.unipd

Accepted 30 August; published on WWW 24 October 2000

Summary

Liver mitochondria from the great green goby *Zosterisessor ophiocephalus* (Pallas) normally exhibit bioenergetic variables (membrane potential 165±7 mV; respiratory control ratio 6.6±0.4; ADP/O ratio 1.85±0.8; means ± S.E.M., *N*=6) and activities of physiological transport systems (phosphate/proton symporter, adenine nucleotide antiporter, Ca^{2+} electrophoretic uniporter) comparable with those of rat liver mitochondria. When incubated in the presence of Ca^{2+} and an inducer agent such as phosphate, these mitochondria undergo a complete collapse of membrane potential accompanied by a large-amplitude swelling of the matrix, influx of sucrose from the incubation medium, release of endogenous Mg^{2+} and K^+ (approximately 90 % of the total) and of preaccumulated Ca^{2+} and oxidation of endogenous pyridine nucleotides. All these phenomena, which are completely eliminated by cyclosporin A and inhibited with different efficacies by Mg^{2+} and spermine, demonstrate that the induction of the permeability transition in this type of mitochondria has characteristics similar to those described in rat liver mitochondria. In contrast, the requirement for very high Ca^{2+} concentrations (greater than 100 μmol l^{-1}) for the induction of the permeability transition represents a very important difference that distinguishes this phenomenon in fish and mammalian mitochondria.

Key words: fish, *Zosterisessor ophiocephalus*, mitochondria, permeability transition, Ca^{2+}, cyclosporin A, Mg^{2+}, spermine.

Introduction

Over the past 20 years, many studies on cellular bioenergetics have focused on the induction of a non-selective solute permeability increase in the inner mitochondrial membrane of Ca^{2+}-loaded mitochondria, termed the membrane permeability transition (MPT). This state results from the opening of a pore that is probably proteinaceous in nature, has a diameter of approximately 2–3 nm and permits the transit of molecules with a molecular mass of 1.5 kDa. This pore behaves as a voltage-dependent channel that is modulated both by the membrane potential and by the matrix pH and is inhibited by cyclosporin A, several divalent and polyvalent cations (Mg^{2+}, polyamines) and ADP (for reviews, see Gunter and Pfeiffer, 1990; Gunter et al., 1994; Zoratti and Szabò, 1995). While its physiological role is not yet understood, the MPT has been correlated with cell death by necrosis (Nieminen et al., 1995) and also constitutes a fundamental step in the signalling cascade leading to apoptosis (Zanzami et al., 1996; Mignotte and Kayssiene, 1998). Indeed, an increasing body of evidence supports the hypothesis of a key role for the MPT as a final common point at which the pathways of many toxic agents converge (Pastorino et al., 1993; Costantini et al., 1995). The MPT leads to a collapse of membrane potential ($\Delta\psi$) and the onset of a bidirectional trafficking of solutes through the inner membrane that, as a first consequence, induces swelling of the matrix.

Our understanding of the MPT is based almost exclusively on studies of mitochondria isolated from rat heart or liver; the literature includes only a few sporadic studies on Ca^{2+}-dependent MPT pore opening in non-mammalian organisms (Szabò et al., 1995; Vianello et al., 1995), and the phenomenon has never been studied in fish. Many studies in aquatic animals do, however, show mitochondrial swelling as a sign of irreversible cell damage after the uptake of toxins (Lemaire et al., 1992; Benedeczky and Nemoskos, 1997). Benedeczky and Nemoskos (1997) have proposed that the appearance of the so-called 'giant mitochondria' could be utilized as a marker for monitoring cell damage by environmental xenobiotics. These osmotic alterations resemble those associated with the MPT *in vitro* which, as mentioned above, strongly compromises the bioenergetic functions of mammalian mitochondria. The aim of the present study was to determine the bioenergetic variables of liver mitochondria isolated from the teleost fish *Zosterisessor ophiocephalus* and to investigate whether the MPT can also be induced in this organism. To our knowledge, this represents the first such analysis performed on fish mitochondria.

Materials and methods

With the exception of the isolation of fish liver mitochondria (FLM), the methods employed in this study have been published previously; modifications to the published methods are specified.

Experimental animals

Specimens of both sexes of the great green goby *Zosterisessor ophiocephalus* (Pallas) (Gobiidae, Perciformes, Teleostei), approximately 2 years old and weighing 50–80 g, were wild-caught in the North Adriatic sea near Chioggia, Italy, and kept in a tank with running sea water at ambient temperature (approximately 18 °C) for 24 h without food.

Preparation and incubation of mitochondria

Fish were anaesthesized with 1–2 % phenoxyethanol and then decapitated. The liver was promptly removed and immediately immersed in an ice-cold isolation medium containing 250 mmol l^{-1} sucrose, 5 mmol l^{-1} Hepes (pH 7.4), 2 mmol l^{-1} EGTA and 5 mmol l^{-1} dithioerythritol (DTE). Bovine serum albumin (5 mmol l^{-1}) was also added to avoid mitochondrial damage by fatty acids or lysophospholipids. The liver tissue was minced, thoroughly rinsed three times with ice-cold medium and then homogenized in 50 ml of the same buffered solution using a Potter homogenizer with a Teflon pestle in an ice-water bath. Mitochondria were then isolated by conventional differential centrifugation as follows. The cell debris, myofibrils, nuclei and other heavy components were removed by sedimentation at 755 ***g*** for 5 min in a Sorvall RC-5B centrifuge. The supernatant was filtered through glass wool, and the mitochondria were then sedimented at 10 800 ***g*** for 10 min. The supernatant was discarded, and the mitochondrial pellet was carefully resuspended in ice-cold isolation medium, sedimented again at 15 800 ***g*** for 5 min, and then resuspended in 250 mmol l^{-1} sucrose; EGTA and DTE were omitted from the final wash and resuspension. The protein content was measured by the biuret method with bovine serum albumin as a standard (Gornall et al., 1949). The resulting mitochondrial suspensions were maintained on ice in washing medium (isolation medium without EGTA and DTE) at protein concentrations of approximately 40 mg ml^{-1}. The preparations had the following ion contents (nmol mg^{-1} protein): Ca^{2+}, 15; Mg^{2+}, 24; K^+, 110; phosphate (P_i), 18.

Incubations were carried out at 20 °C with 1 mg ml^{-1} of mitochondrial protein in the following standard medium: 200 mmol l^{-1} sucrose, 10 mmol l^{-1} Hepes (pH 7.4), 5 mmol l^{-1} succinate, 1.25 μmol l^{-1} rotenone and 1 mmol l^{-1} P_i. Sodium salts were used. In some experiments, sucrose was substituted with 100 mmol l^{-1} NaCl. Other additions are indicated in the description of specific experiments.

Assessment of mitochondrial integrity and function

Membrane potential (Δψ), respiratory control ratio (RCR), ADP/O ratio, [^{14}C]ADP transport and Ca^{2+} movement were utilized to evaluate the bioenergetic variables of energized FLM. Swelling, [^{14}C]sucrose transport, release of endogenous Mg^{2+} and K^+ and of accumulated Ca^{2+}, oxidation of pyridine nucleotides and Δψ were measured to monitor the increase in non-specific permeability of the inner mitochondrial membrane.

The membrane potential (Δψ) was measured by assessing the distribution of the lipophilic cation tetraphenylphosphonium (TPP^+) across the mitochondrial membrane with an ion-selective electrode specific for TPP^+, prepared according to Kamo et al. (1979), with a calomel reference electrode (Radiometer K401). In this method, the electrode potential is linear with respect to the logarithm of the TPP^+ activity, with a slope of 58 mV, according to the Nernst equation and the law of mass conservation, and assuming an inner mitochondrial volume of 1.4 l mg^{-1} protein, calculated from the distributions of [^{14}C]sucrose and ^3H_2O according to Palmieri and Klingenberg (1979). TPP^+ was added at a concentration of 2 μmol l^{-1} to allow accurate measurements while avoiding toxic effects on the H^+-ATPase (Jensen and Gunter, 1984) and Ca^{2+} movements (Karadyov et al., 1986). Δψ measured with the TPP^+ electrode was calibrated using the equation: $\Delta\psi=(\Delta\psi_{electrode}-66.16)/0.92$, as proposed by Jensen et al. (1986).

The respiratory control ratio was calculated by determining the difference in rates of oxygen uptake between respiratory state 4 (in the absence of 300 μmol l^{-1} ADP) and state 3 (in the presence of 300 μmol l^{-1} ADP) using a Clark oxygen electrode (Yellow Springs Instrument Co. Inc.) in a closed, thermostatically controlled vessel with a magnetic stirrer, coupled to a Perkin-Elmer 561 recorder (Estabrook et al., 1967).

The ADP/O ratio was calculated by dividing the concentration of added ADP by the corresponding oxygen uptake during respiratory state 3.

Ca^{2+} movements were followed with a Ca^{2+}-selective electrode (Radiometer F2112) and a calomel reference electrode (Radiometer K401) in the same vessel used for oxygen uptake measurements.

A centrifugal-filtration method (Toninello et al., 1988) was used to measure the mitochondrial uptake of P_i, [^{14}C]ADP and [^{14}C]sucrose and the release of Mg^{2+}, K^+ and Ca^{2+}. Centrifugal filtrations were performed in an Eppendorf 5415 C microfuge using tubes containing 150 μl of 12.5 % (v/v) sucrose placed on the bottom and 400 μl of a mixture of silicone oils [AR100/AR150 (2:1); Wacker-Chemie GmbH, Munich, Germany] carefully layered on top. Samples (1.5 ml) were periodically withdrawn from incubation mixtures and carefully layered onto the silicone oil; the mitochondria were then rapidly sedimented in the microfuge, which generates approximately 15 000 ***g*** and sediments mitochondria within 15–20 s. To ensure complete sedimentation, centrifugation was continued for more than 1 min. The upper layer of the supernatant was removed and utilized for cation efflux measurements. The release of Mg^{2+}, K^+ and Ca^{2+} was determined by atomic absorption measurements in a Perkin-Elmer 1100 B spectrometer. The walls of the tubes and the surface of the silicone oil layer were washed three times with incubation medium, and the silicone oil layer was then

removed as well. The mitochondrial pellet was solubilized with the sucrose of the lower layer and utilized for P_i, [^{14}C]ADP and [^{14}C]sucrose measurements.

Phosphate content was determined by the colorimetric method of Baginski et al. (1967). ADP transport was measured according to Toninello et al. (1990). After preincubation of FLM for 1 min, the reaction was started by the addition of 500 μmol l^{-1} [^{14}C]ADP (1.85 MBq $mmol^{-1}$) and stopped after 30 min by the addition of 25 μmol l^{-1} carboxyatractyloside. Samples of 1.5 ml were withdrawn and subjected to centrifugal filtration as described for the determination of P_i and cations. The pellet was rinsed twice with 1 ml of standard medium, solubilized with a mixture of 1 mmol l^{-1} Na-EDTA, 100 μmol l^{-1} NaCl and 0.9 % sodium deoxycholate, and the radioactivity was measured by liquid scintillation counting in a Beckman LS-100C scintillation counter.

Sucrose permeation was determined according to the method of Crompton and Costi (1988) in standard medium containing [^{14}C]sucrose (18.5 kBq $mmol^{-1}$). Samples of 1.5 ml were periodically withdrawn and treated with 10 mmol l^{-1} EGTA to seal the inner membrane of the FLM and thereby to block any solute movement. The FLM were then pelleted by centrifugation and solubilized, and radioactivity was monitored as described above.

The redox state of endogenous pyridine nucleotides was followed fluorometrically in an Aminco-Bowman 4-8202 spectrofluorometer with excitation at 354 nm and emission at 462 nm (Moore et al., 1987). The experimental protocol was identical to that used to monitor swelling (see above).

Results

The results reported in Fig. 1A show that FLM incubated in standard medium exhibit a value of Δψ of approximately 160 mV. Addition of P_i provokes an increase in Δψ to approximately 170 mV; subsequent addition of ADP triggers a transient decline in Δψ, which then returns to approximately 170 mV (curve a). The increase in Δψ upon addition of P_i is due to a lowering of pH caused by the activity of the electroneutral P_i/H^+ symporter. The other variations in Δψ derive from a state 4 to state 3 transition reflecting energy transduction following ADP addition. Oligomycin is known to block the activity of ATP synthase by closing F_0 channels and promoting a Gibbs energy shift from phosphorylation potential

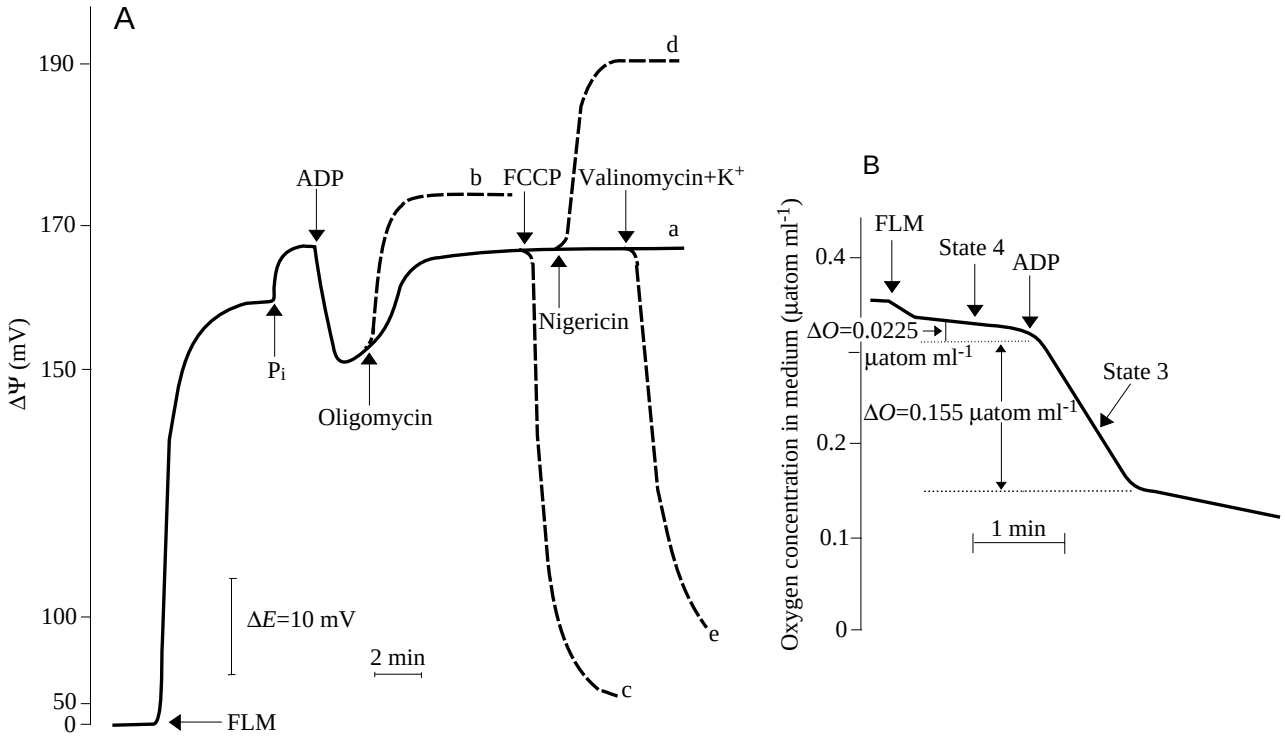

Fig. 1. Measurement of variations in membrane potential (Δψ) (A) and oxygen uptake (B) during the transitions among different respiratory states. (A) Fish liver mitochondria (FLM) were added to standard medium lacking inorganic phosphate (P_i), in the conditions described in Materials and methods. P_i (1 mmol l^{-1}) was added after 5 min, immediately followed by 300 μmol l^{-1} ADP (curve a). Other subsequent additions were as follows: 5 μmol l^{-1} oligomycin (curve b), 200 nmol l^{-1} FCCP (curve c), 500 nmol l^{-1} nigericin (curve d) and 300 nmol l^{-1} valinomycin plus 5 mmol l^{-1} KCl (curve e). Five additional experiments exhibited the same trend. The mean value of Δψ in the presence of P_i was 165±7 mV (mean ± S.E.M., N=6). (B) FLM were added to standard medium; 300 μmol l^{-1} ADP was added at the point indicated on the curve. The respiratory control ratio (RCR) was calculated as the ratio between the respiratory rates measured in state 3 and in state 4, and yielded a value of 6.9. The ADP/O value was 1.93. A typical experiment is illustrated; the mean values for RCR measured in six experiments was 6.6±0.4 and the mean ADP/O was 1.85±0.8 (means ± S.E.M., N=6). ΔE, electrode potential; ΔO, rate of oxygen consumption.

to electrochemical gradient. The addition of oligomycin causes $\Delta\psi$ to rise above 170 mV (curve b). In contrast, complete de-energization is observed upon addition of the uncoupler carbonyl cyanide-*p*-trifluorometoxyphenilhydrazone (FCCP), which induces a sudden collapse of $\Delta\psi$ to a minimal value by dissipating the electrochemical gradient as heat (curve c). The addition of the ionophore nigericin, which promotes exchange between endogenous K^+ and exogenous H^+, causes a complete collapse of ΔpH, resulting in an increase in $\Delta\psi$ to a maximum value of approximately 190 mV (curve d). The ionophore valinomycin, however, induces the electrophoretic import of K^+ and causes the collapse of $\Delta\psi$ (curve e) accompanied by an increase in ΔpH (not shown).

Fig. 1B describes the measurement of RCR and ADP/O. The addition of a limiting amount of ADP (300 μmol l^{-1}) to FLM that are oxidizing succinate in the presence of rotenone and P_i at a rate of 0.0025 μatom min^{-1} (state 4 respiration) provokes a strong transitory increase in oxygen uptake to a rate of 0.155 μatom min^{-1} (state 3 respiration). When ADP is completely phosphorylated to ATP, the rate of oxygen uptake returns to the preceding state 4. The RCR is 6.6±0.4, and the ADP/O ratio is 1.85±0.8 (means ± S.E.M., *N*=6), demonstrating excellent coupling between ATP synthesis and oxygen uptake in FLM.

Fig. 2 shows the kinetics of the transport of both ADP and P_i into the mitochondrial matrix. The results demonstrate that FLM accumulate approximately 10 nmol [^{14}C]ADP mg^{-1} protein and 21 nmol P_i mg^{-1} protein over the 30 min incubation period. The addition of carboxyatractyloside, an inhibitor of the adenine nucleotide translocase, and mersalyl, an inhibitor of the P_i/H^+ symporter, greatly reduces ADP and P_i transport. The residual uptake of ADP and P_i after 1 min of incubation in the presence of the inhibitors reflects the entry of the two metabolites into the intermembrane space.

As shown in Fig. 3, the addition of 100 μmol l^{-1} Ca^{2+} to the standard medium results in partial uptake of the cation by the FLM to a concentration of approximately 50 μmol l^{-1}. Addition of P_i strongly enhances Ca^{2+} transport, resulting in a reduction in the external concentration to 900 nmol l^{-1} (curve a), while the subsequent addition of ruthenium red, an inhibitor of this uptake, induces a gradual efflux of the cation, until an external concentration of 50 μmol l^{-1} is reached (curve b). Addition of FCCP (curves c) or valinomycin plus K^+ (curve d) induces the release of Ca^{2+} at higher rates and than that observed with ruthenium red. These distinct responses are due to different pathways of Ca^{2+} efflux: ruthenium red, under energized conditions, induces Ca^{2+} efflux *via* the Ca^{2+}/H^+ antiporter, while FCCP (curve c) and valinomycin plus K^+ (curve d)

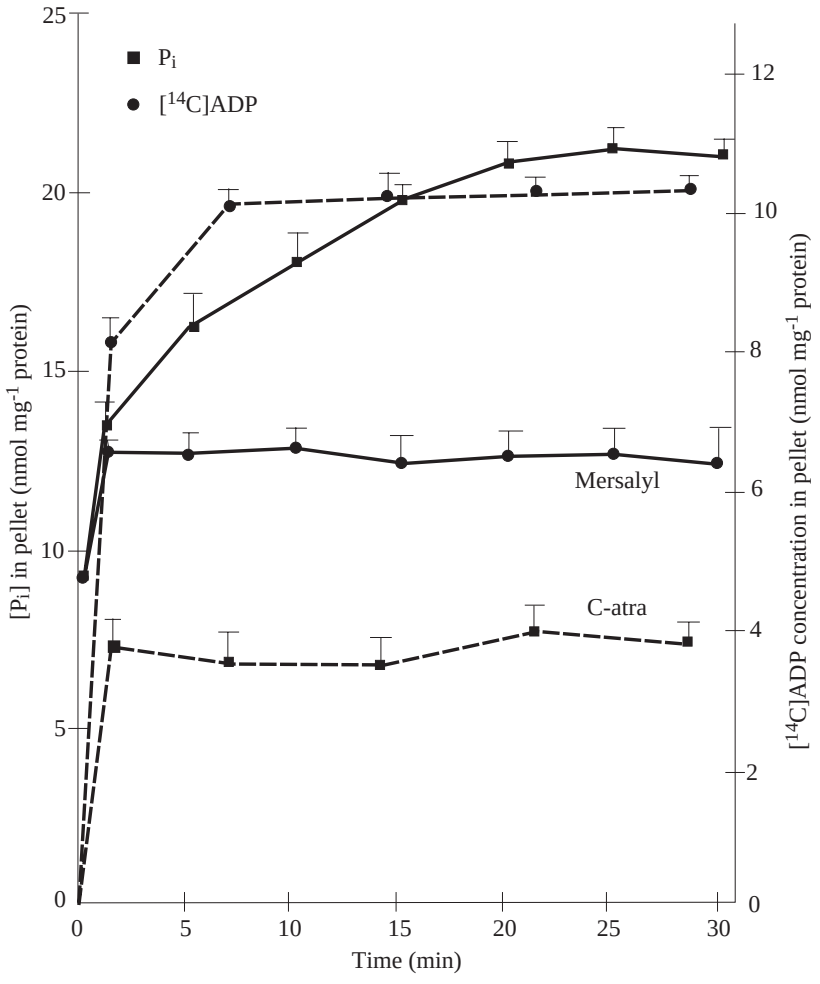

Fig. 2. Phosphate (P_i) and ADP uptake by fish liver mitochondria (FLM). Measurements were performed in two separate vessels. P_i uptake was measured by incubating FLM in standard medium as described in Materials and methods; ADP uptake was measured by incubating FLM in standard medium lacking P_i and supplemented with [^{14}C]ADP (500 μmol l^{-1}; 1.85 MBq $mmol^{-1}$); 10 μmol l^{-1} mersalyl and 5 μmol l^{-1} carboxyatractyloside (C-atra) were added as indicated. The results represent the mean value + S.E.M. of seven experiments. The endogenous content of P_i was 9 nmol mg^{-1} protein.

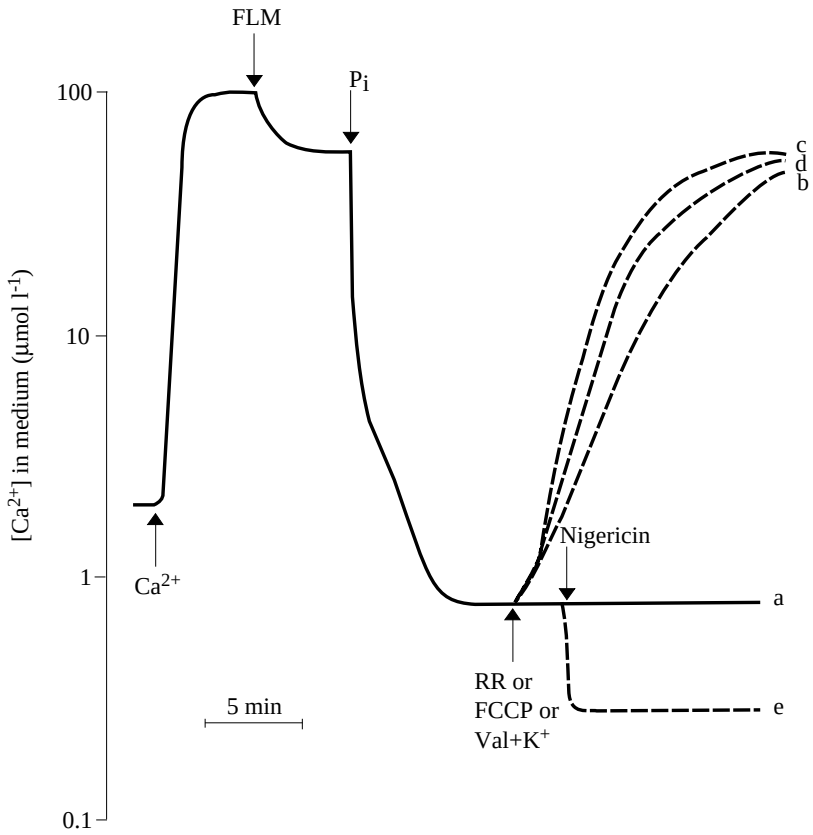

Fig. 3. Ca^{2+} movements in fish liver mitochondria (FLM). FLM were added to standard medium as in Fig. 1A in the presence of 100 μmol l^{-1} Ca^{2+}, followed by the addition of 1 mmol l^{-1} P_i (curve a). Where indicated, 1 μmol l^{-1} ruthenium red (RR) (curve b), 200 nmol l^{-1} FCCP (curve c), 300 nmol l^{-1} valinomycin plus 5 mmol l^{-1} KCl (Val+K^+) (curve d) or 500 nmol l^{-1} nigericin (curve e) was added separately. The measurements were performed using a Ca^{2+} electrode. The assays were performed seven times with comparable results.

collapse Δψ (see also Fig. 1A) and induce Ca^{2+} efflux *via* the reverse of the electrophoretic uniporter. The addition of nigericin, which substantially increases Δψ (see Fig. 1A), further enhances Ca^{2+} uptake (curve e) with respect to that observed in the presence of P_i (curve a).

The addition of 150 μmol l^{-1} Ca^{2+} to mitochondria suspended in standard medium induces an initial sudden, transitory collapse of Δψ, followed by a second slower, but irreversible, decrease (Fig. 4, curve a). The presence of cyclosporin A (curve b), spermine (curve c) or Mg^{2+} (curve d) shortens the transitory collapse of Δψ and completely prevents its subsequent decrease, maintaining it at the control level (approximately 160 mV). The Δψ collapse induced by the addition of 150 μmol l^{-1} Ca^{2+} is accompanied by a time-dependent decrease in absorbance at 540 nm of approximately 0.45 units (Fig. 5A, curve a), indicating the occurrence of colloid-osmotic swelling of the mitochondrial matrix. The presence of cyclosporin A almost completely abolishes this effect (Fig. 5A, curve b), and spermine (curve c) and Mg^{2+} (curve d) decrease it slightly less effectively. As demonstrated in Fig. 5B (curve a), this osmotic effect is due to the entry of 75 nmol sucrose mg^{-1} protein into the matrix space. The presence of cyclosporin A (Fig. 5B, curve b), spermine (curve c) or Mg^{2+} (curve d) also exerts an inhibitory effect under these conditions. The addition of EGTA at any time immediately blocks both mitochondrial swelling (see inset in Fig. 5A) and sucrose entry (data not shown), thus demonstrating that the observed phenomena are linked to Ca^{2+} transport. The accumulation of Ca^{2+} and P_i in FLM also promotes the efflux of endogenous Mg^{2+}, with approximately 80 % released in 20 min (Fig. 6, curve a); this efflux is strongly inhibited by cyclosporin A (Fig. 6, curve b) and more weakly inhibited by spermine (curve c).

The results reported in Fig. 7 show that, in parallel with Mg^{2+} release (see Fig. 6), the entry of Ca^{2+} plus P_i into FLM induces an efflux of approximately 90 % of the endogenous K^+ after 20 min of incubation (see curve a, Fig. 6A). In the presence of quinine, an inhibitor of the K^+/H^+ exchanger, K^+ is not retained (Fig. 6A), thus demonstrating that its efflux is not dependent on this exchanger. After the same period, approximately 100 nmol Ca^{2+} mg^{-1} protein is also released, but 50 nmol mg^{-1} protein remains within the mitochondria (curve a, Fig. 6B). In fact, in contrast to rat liver mitochondria, FLM release their accumulated Ca^{2+} very slowly. Furthermore, it is noteworthy that FLM take up approximately 50 nmol Ca^{2+} mg^{-1} protein in the presence of ruthenium red or FCCP (Fig. 7B).

Cyclosporin A (Fig. 7B, curve b) and spermine (curve c) exert inhibitory effects on K^+ efflux similar to those observed with Mg^{2+} (curve d), except that Mg^{2+} exerts a weaker protective effect than the polyamine. The presence of these inhibitors prevents any efflux of accumulated Ca^{2+}.

All the effects reported above induced by Ca^{2+} and P_i are also accompanied by the oxidation of endogenous pyridine nucleotides (Fig. 8, curve a). This event is strongly inhibited by cyclosporin A (Fig. 8, curve b) and Mg^{2+} (curve d),

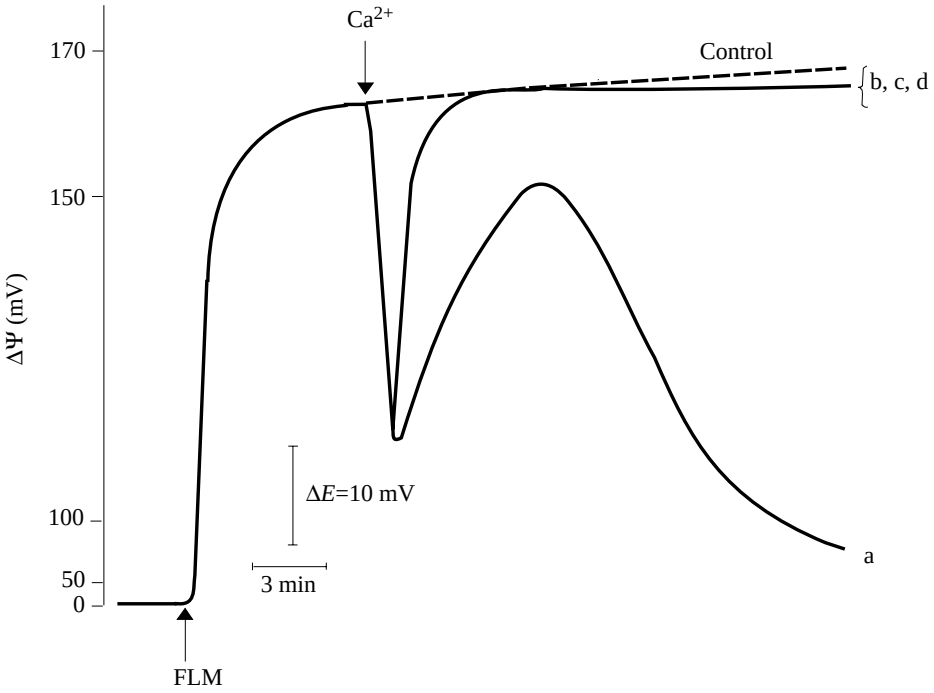

Fig. 4. Effects of Ca^{2+} plus phosphate on the membrane potential of fish liver mitochondria (FLM): protection by cyclosporin A, spermine and Mg^{2+}. FLM were added to standard medium as described in Materials and methods in the presence of $1\,\mu mol\,l^{-1}$ TPP^+ and either $1\,\mu mol\,l^{-1}$ cyclosporin A (curve b), $100\,\mu mol\,l^{-1}$ spermine (curve c) or $1\,mmol\,l^{-1}$ Mg^{2+} (curve d). Additions of $150\,\mu mol\,l^{-1}$ Ca^{2+} (curves a–d) were made where indicated. The dashed line represents FLM in the absence of Ca^{2+} (control). The assays were performed seven times with comparable results. ΔE, electrode potential.

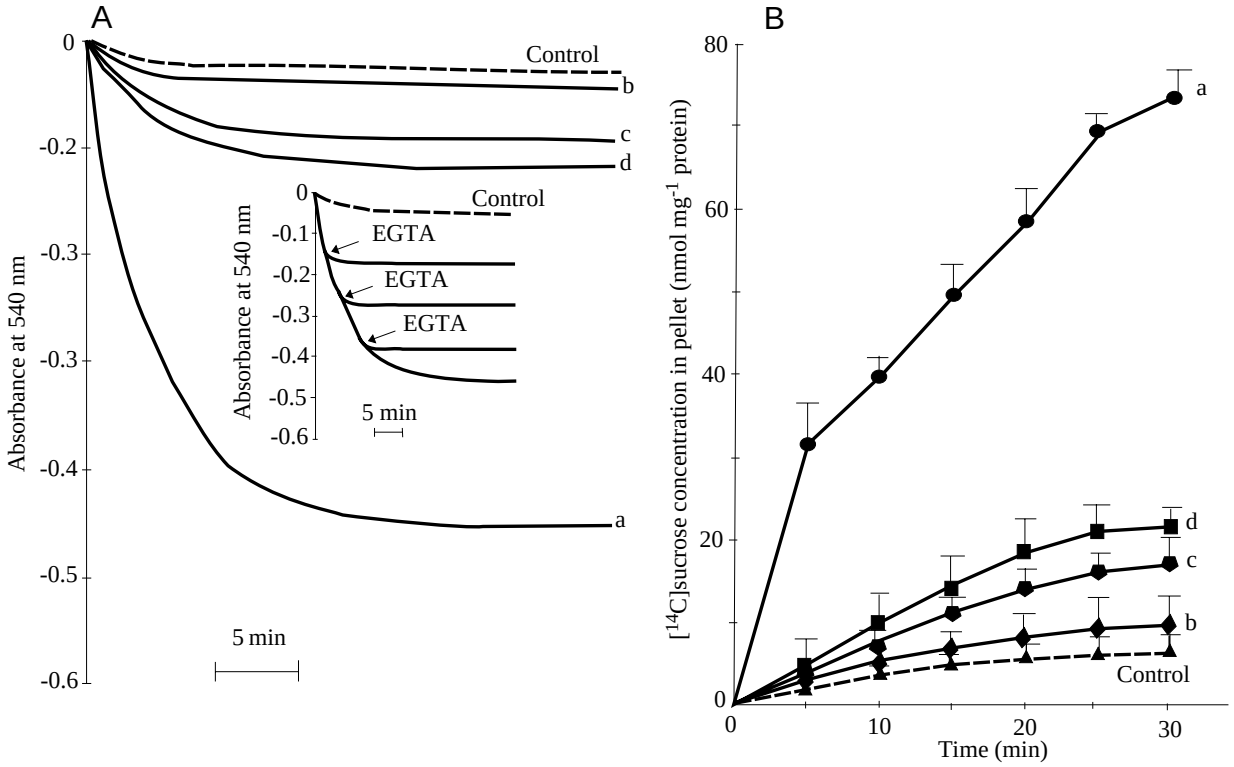

Fig. 5. Effects of cyclosporin A, spermine and Mg^{2+} on mitochondrial swelling (A) and sucrose permeation (B) induced by Ca^{2+} and P_i. Fish liver mitochondria (FLM) were incubated in standard medium in the presence of $150\,\mu mol\,l^{-1}$ Ca^{2+} (curves a–d), and $1\,\mu mol\,l^{-1}$ cyclosporin A (curve b), $100\,\mu mol\,l^{-1}$ spermine (curve c) or $1\,mmol\,l^{-1}$ Mg^{2+} (curve d) was added as indicated. The inset in A reports the effects of $1\,mmol\,l^{-1}$ EGTA added at different times to FLM incubated in standard medium plus $150\,\mu mol\,l^{-1}$ Ca^{2+}. The assays were performed seven times with comparable results. (B) [^{14}C]sucrose ($18.5\,kBq\,mmol^{-1}$) was added to the medium. The results represent the mean values + S.E.M. of seven experiments. The dashed line represents FLM in the absence of Ca^{2+} (control). Additions for curves a–d are as in A.

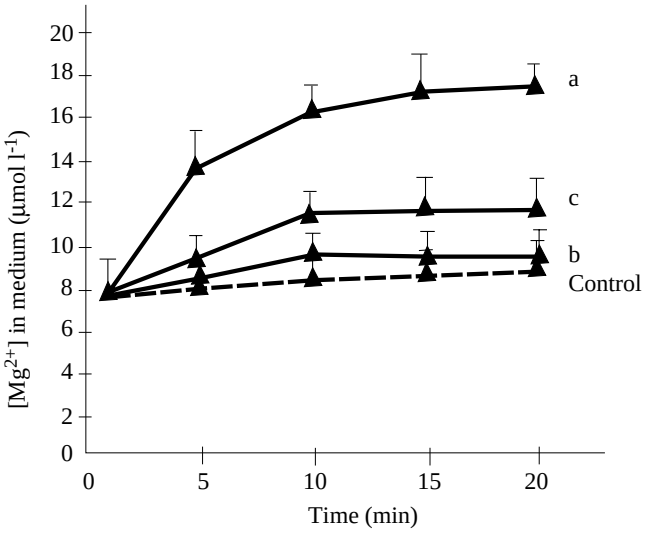

Fig. 6. Effects of cyclosporin A and spermine on the efflux of endogenous Mg^{2+} induced by Ca^{2+} and P_i. Fish liver mitochondria (FLM) were incubated in standard medium in the presence of 150 μmol l^{-1} Ca^{2+} (curves a–c) and either 1 μmol l^{-1} cyclosporin A (curve b) or 100 μmol l^{-1} spermine (curve c) was added as indicated. The dashed line represents FLM in the absence of Ca^{2+} (control). The values are means + S.E.M. of seven experiments.

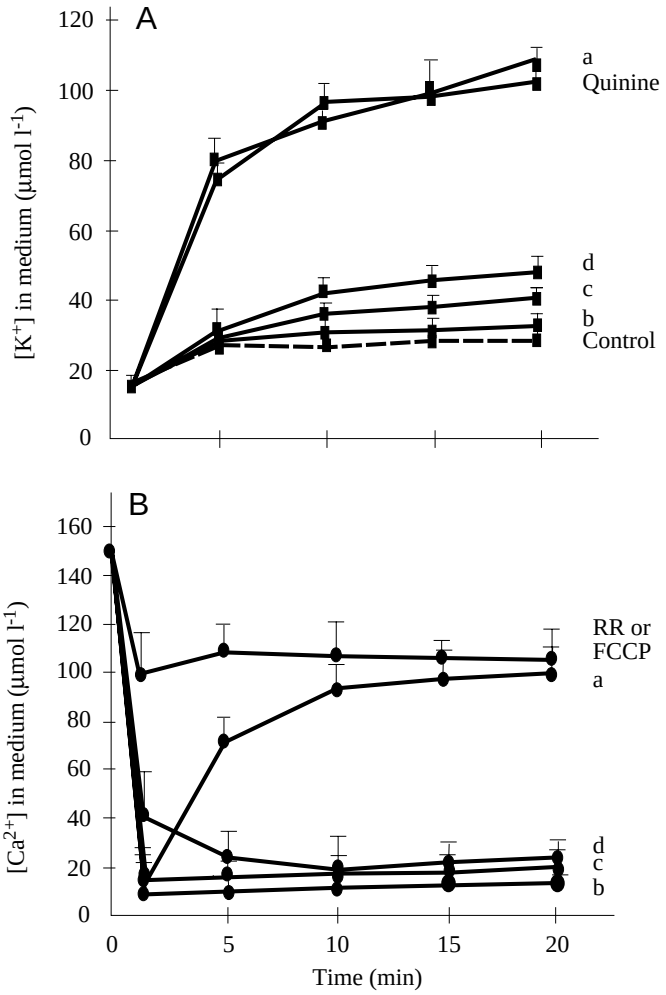

Fig. 7. Effects of cyclosporin A, spermine and Mg^{2+} on the efflux of endogenous K^+ (A) and Ca^{2+} (B) induced by Ca^{2+} and P_i. Fish liver mitochondria (FLM) were incubated in standard medium in the presence of 150 μmol l^{-1} Ca^{2+} (curves a–d), and 1 μmol l^{-1} cyclosporin A (curve b), 100 μmol l^{-1} spermine (curve c) or 1 mmol l^{-1} Mg^{2+} (curve d) was added as indicated. Quinine (100 μmol l^{-1}; A) and either 1 μmol l^{-1} ruthenium red (RR) or 200 nmol l^{-1} FCCP (B) was also added. The dashed line represents FLM in the absence of Ca^{2+} (control). The values are means + S.E.M. of 7 experiments.

resulting in an increase in NADH/NAD^+ ratio accompanied by an increase in fluorescence; spermine does not exhibit this protective effect (Fig. 8, curve c).

Discussion

The bioenergetic functions of liver mitochondria isolated from *Z. ophiocephalus* are comparable with those of rat liver mitochondria. This statement is supported (i) by the Gibbs energy changes induced upon addition of ADP, oligomycin, valinomycin or FCCP to energized mitochondria (Fig. 1), (ii) by the $\Delta\psi \rightarrow \Delta pH$ shift promoted by the addition of P_i or nigericin, (iii) by the high values of RCR and ADP/O, and (iv) by the characteristics of Ca^{2+} transport, i.e. electrophoretic influx mediated by P_i and electroneutral efflux blocked by ruthenium red (Fig. 3). Furthermore, the strong inhibitory effects exhibited by mersalyl on the P_i symporter, by carboxyatractyloside on the adenine nucleotide translocase (Fig. 2) and by ruthenium red on the Ca^{2+} uniporter (Fig. 3) confirm the presence of these transport systems in fish mitochondria.

As described in the Introduction, energy-dependent Ca^{2+} transport, if associated with the entry of an inducer agent such as P_i into the matrix, promotes MPT in mammalian mitochondria. Membrane energization therefore appears to be a prerequisite to the induction of this phenomenon. Fish liver mitochondria are able to transduce energy with the same efficiency as mammalian mitochondria (see Fig. 1). When incubated in the presence of high concentrations of Ca^{2+} and P_i, FLM undergo a collapse of $\Delta\psi$ (Fig. 4) accompanied by colloid-osmotic alterations (Fig. 5), cation efflux (Figs 6, 7) and pyridine nucleotide oxidation (Fig. 8). As previously reviewed (Zoratti and Szabò, 1995), these effects are characteristic of MPT induction. The observed inhibitory actions of EGTA, cyclosporin A, Mg^{2+} and spermine (Figs 4–8) further confirm that MPT induction can indeed occur in FLM. Because of its physiological importance, P_i was used as an inducer in the present experiments, but other agents, such as pro-oxidants, can substitute for P_i in the above assays (data not shown).

It must be emphasized that the MPT in fish displays some differences from that observed in rats. The results reported in Fig. 5 show that the maximum absorbance change, indicative of mitochondrial swelling, is approximately 0.5 unit in FLM,

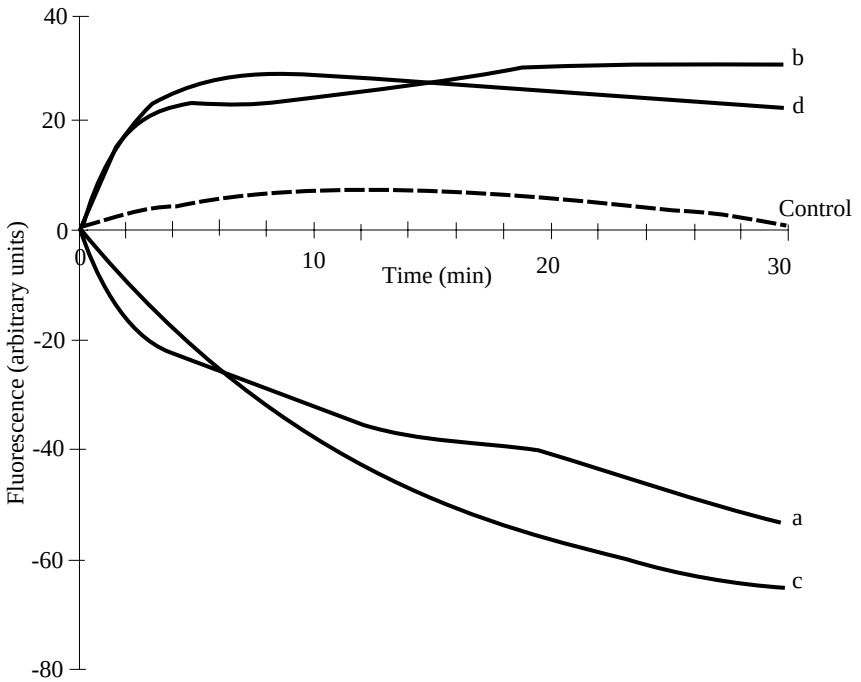

Fig. 8. Effects of cyclosporin A, spermine and Mg^{2+} on pyridine nucleotide oxidation induced by Ca^{2+} and P_i. Fish liver mitochondria (FLM) were incubated in standard medium in the presence of 150 μmol l^{-1} Ca^{2+} (curves a–d), and 1 μmol l^{-1} cyclosporin A (curve b), 100 μmol l^{-1} spermine (curve c) or 1 mmol l^{-1} Mg^{2+} (curve d) was added as indicated. The dashed line represents FLM in the absence of Ca^{2+} (control). A typical experiment is illustrated; six additional experiments gave comparable results.

compared with the 1 unit normally observed in rat liver mitochondria. Furthermore, sucrose uptake is approximately 60–70 nmol mg^{-1} protein in FLM, and approximately 200 nmol mg^{-1} protein in rat liver mitochondria (Rigobello et al., 1993). Although the origin of these differences is unknown, one possibility is that FLM contain a smaller number of cristae, which limits the increase in stretching and in volume. Electron microscopy studies currently under way in our laboratory will verify this hypothesis. Another peculiarity is that the induced efflux of Ca^{2+} is slow and incomplete (Fig. 7B). In this regard, it must be taken into account that 40–50 nmol Ca^{2+} mg^{-1} protein is taken up by FLM in the presence of FCCP or ruthenium red, which blocks the uptake of Ca^{2+} into the matrix space. The reduced efflux is probably due to the presence of low-affinity Ca^{2+}-binding sites outside the matrix space that are able to retain the cation bound to the organelles.

The loss of intramitochondrial ions (Figs 6, 7) is not always an indicator of pore opening, because it can also result from the activation of specific transporters (Garlid, 1980; Jung and Brierley, 1994). However, the lack of inhibition of K^+ efflux by quinine, a specific inhibitor of the K^+/H^+ antiporter (Fig. 7A), indicates that this particular mechanism is not responsible for the release of K^+, thus validating the hypothesis of MPT induction.

The conclusion that the observed events are due to the MPT is confirmed by the inhibitory effect exhibited by cyclosporin A (see Figs 4–8). This immunosuppressant cyclic peptide represents the most powerful MPT inhibitor in common use, and it is equally effective when different types of inducers are employed. The protective action of cyclosporin A is a very important parameter for identifying pore opening (Crompton and Costi, 1988; Broekemeier et al., 1989); the high specificity of its interaction enables us to exclude the possibility that the observed events reflect non-specific alterations in the lipid bilayer. Moreover, additional assays verified the protective effects of spermine and Mg^{2+} which, unlike cyclosporin A, are of physiological relevance, although the mechanism of their inhibition is not known. Spermine and Mg^{2+} have limited efficacies, as reflected by the fact that they must be added at 100- and 1000-fold higher concentrations, respectively, than cyclosporin A. At these concentrations, spermine and Mg^{2+} completely prevent the decrease in $\Delta\psi$ (Fig. 4), the efflux of intramitochondrial Mg^{2+} and K^+ and the efflux of preaccumulated Ca^{2+} (Figs 6, 7). Swelling is considerably reduced in the presence of these cations (Fig. 5). Like cyclosporin A, Mg^{2+} completely inhibits the oxidation of pyridine nucleotides (Fig. 8). The increase in the NADH/NAD^+ ratio observed with both these inhibitors (see fluorescence increase in Fig. 8) must be attributed to a further reduction in levels of endogenous nucleotides due to the presence of rotenone, which blocks NADH oxidation. The failure of spermine to increase the NADH/NAD^+ ratio is unexpected, as it shows a similar effect to those of Mg^{2+} and cyclosporin A in rat liver mitochondria. This phenomenon is difficult to explain. Although spermine is not able to prevent MPT completely, it does exhibit an inhibitory effect (see Figs 4–7), which should also be evident at the level of pyridine nucleotide oxidation. One possibility is that pyridine nucleotide oxidation in FLM is not directly linked to MPT induction and that spermine is not able to interact with the critical site(s) responsible for NAD(P)H oxidation.

Although the physiological role of the MPT is not known, much evidence supports the hypothesis that it represents a final common point at which many toxic agents and pathological conditions may converge. Data reported in the literature

support a connection between the MPT and the toxic effects of several agents, including 1-methyl-4-phenylpyridinium (Snyder et al., 1992), *t*-butylhydroperoxide (Kass et al., 1992; Imberti et al., 1993), cumene hydroperoxide and 3,5-dimethyl-*N*-acetyl-*p*-benzoquinone immine (Kass et al., 1992), and in the anoxic and cyanide-induced cell death of primary cultures of hepatocytes (Pastorino et al., 1993).

The main difference between the MPT in fish and rat liver mitochondria revealed in the present study is the higher concentration of Ca^{2+} required to induce the phenomenon in fish mitochondria: FLM need a Ca^{2+} concentration higher than 100 μmol l^{-1} for the induction of MPT, while approximately 20–50 μmol l^{-1} is sufficient for rat liver mitochondria (Gunter and Pfeiffer, 1990; Zoratti and Szabò, 1995). This difference could be ascribed to a lower binding affinity for Ca^{2+} at the level of the critical site(s) present in the pore-forming structures of FLM and could represent a defence mechanism of fish living in polluted water.

Interestingly, *Z. ophiocephalus* displays both high environmental tolerance and considerable resistance to various pollutants. It is among the few teleost fishes inhabiting the Venice Lagoon all year round and can withstand large seasonal fluctuations in water temperature, salinity and oxygenation level. Being a bottom-dweller, it burrows into the sediments, where it can resist high concentrations of accumulated heavy metals, polycyclic aromatic hydrocarbons, polychlorobiphenyls, pesticides and other contaminants, all of which are present in the Venice Lagoon (Pulsford et al., 1995). Thus, it is conceivable that the lower mitochondrial MPT inducibility and attenuated colloid-osmotic alterations associated with the MPT may provide an adaptation to a particularly harsh habitat.

It is of interest, however, that spermine and Mg^{2+} exerted slightly diminished protective effects in FLM at the level of events connected with MPT induction, such as osmotic alterations (Fig. 5A,B) and Mg^{2+} (Fig. 6) and K^+ (Fig. 7A) efflux. A simple explanation for this observation could be that spermine- and Mg^{2+}-binding sites in the pore-forming structures of FLM assume a conformation that reduces the rate of binding compared with that of rat liver mitochondria. This would cause a reduction in the protective effect due to delayed pore closure, resulting in continued solute traffic, albeit very limited, across the inner membrane. The fact that spermine and Mg^{2+} maintain $\Delta\psi$ at normal levels (Fig. 4) and do not induce the release of accumulated Ca^{2+} (Fig. 7B) is in agreement with the hypothesis that pore closure, although delayed, is complete after 10–12 min of incubation. Subsequently, the mitochondria regain their insulating properties and are able to reaccumulate both TPP^+ (the probe for measurement) and Ca^{2+} lost during the temporary pore opening.

In conclusion, the demonstration that Ca^{2+} and P_i are able to induce MPT in FLM opens new possibilities for exploring the mechanism of action of toxic agents in aquatic environments.

We are grateful to Mr Mario Mancon for his skilful technical assistance and Professor Laura Tallandini for helpful discussion and suggestions.

References

Baginsky, E. S., Foa, P. P. and Zak, B. (1967). Determination of phosphate: study of labile organic phosphate interference. *Clin. Chim. Acta* **15**, 155–158.

Benedeczky, I. and Nemoskos, J. (1997). Giant mitochondria as possible bioindicators of environmental injuries in fish liver. *Path. Oncol. Res*. **3**, 20–25.

Broekemeier, K. M., Dempsey, M. E. and Pfeiffer, D. R. (1989). Cyclosporin A is a potent inhibitor of the inner membrane permeability transition in liver mitochondria. *J. Biol. Chem.* **264**, 7826–7830.

Costantini, P., Petronilli, V., Colonna, R. and Bernardi, P. (1995). On the effects of paraquat on isolated mitochondria. Evidence that paraquat causes opening of the cyclosporin A-sensitive permeability transition pore synergistically with nitric oxide. *Toxicol.* **99**, 77–88.

Crompton, M. and Costi, A. (1988). Kinetic evidence for a heart mitochondrial pore activated by Ca^{2+}, inorganic phosphate and oxidative stress. A potential mechanism for mitochondrial dysfunction during cellular Ca^{2+} overload. *Eur. J. Biochem.* **178**, 489–501.

Estabrook, R. W. (1967). Mitochondrial respiratory control and the polarographic measurement of ADP/O ratio. *Meth. Enzymol.* **10**, 41–47.

Garlid, K. D. (1980). On the mechanism of regulation of the mitochondrial K^+/H^+ exchanger. *J. Biol. Chem*. **255**, 11273–11279.

Gornall, A. G., Bardawill, C. J. and David, M. M. (1949). Determination of serum proteins by means of the biuret method. *J. Biol. Chem.* **177**, 751–766.

Gunter, T. E., Gunter, K. K., Sheu, S. and Gavin, C. E. (1994). Mitochondrial calcium transport: physiological and pathological relevance. *Am. J. Physiol.* **267**, C313–C339.

Gunter, T. E. and Pfeiffer, D. R. (1990). Mechanisms by which mitochondria transport calcium. *Am. J. Physiol.* **258**, C755–C786.

Imberti, R., Nieminen, A. L., Herman, B. and Lemasters, J. J. (1983). Mitochondrial and glycolytic dysfunction in lethal injury to hepatocytes by *t*-butylhydroperoxide. Protection by fructose, cyclosporin A and trifluoperazine. *J Pharmac. Exp. Ther*. **265**, 392–400.

Jensen, B. D., Gunter, K. K. and Gunter, T. E. (1986). The efficiencies of the component steps of oxidative phosphorylation. II. Experimental determination of the efficiencies in mitochondria and examination of the equivalence of membrane potential and pH gradient in phosphorylation. *Arch. Biochem. Biophys*. **248**, 305–323.

Jensen, B. D. and Gunter, T. E. (1984). The use of tetraphenylphosphonium (TPP^+) to measure membrane potentials in mitochondria: membrane binding and respiratory effects. *Biophys. J*. **45**, 92 (abstr.).

Jung, D. W. and Brierley, G. P. (1994). Magnesium transport by mitochondria. *J. Bioenerg. Biomembr*. **26**, 527–535.

Kamo, N., Muratsugu, M., Hongoh, R. and Kobatake, Y. (1979). Membrane potential of mitochondria measured with an electrode sensitive to tetraphenylphosphonium and relationship between proton electrochemical potential and phosphorylation potential in steady state. *J. Membr. Biol.* **49**, 105–121.

Karadyov, J. S., Kudzina, L. and Yu Zinchenko, V. P. (1986). TPP^+ inhibits Na^+-stimulated Ca^{2+} efflux from brain mitochondria. *Cell Calcium* **7**, 115–119.

Kass, G. E. N., Juedes, M. J. and Orrenius, S. (1992). Cyclosporin A protects hepatocytes against prooxidant-induced cell killing. A study on the role of mitochondrial Ca^{2+} cycling in cytotoxicity. *Biochem. Pharmac*. **44**, 1995–2003.

Lemaire, P., Berhaut, J., Lemaire, G. S. and Lefaurie, M. (1992). Ultrastructure changes induced by benzo(a)pyrene in sea bass (*Dicentrarchus labrax*) liver and intestine: importance of the intoxication route. *Env. Res.* **57**, 59–72.

Mignotte, B. and Kayssiene, J. L. (1998). Mitochondria and apoptosis. *Eur. J. Biochem*. **252**, 1–15.

Moore, G., Rossi, L., Nicotera, P., Orrenius, S. and O'Brien, P. (1987). Quinone toxicity in hepatocytes: studies on mitochondrial Ca^{2+} release induced by benzoquinone derivatives. *Arch. Biochem. Biophys*. **259**, 283–295.

Nieminen, A. L., Saylor, A. K., Tesfai, S. A., Herman, B. and Lemasters, J. J. (1995). Contribution of the mitochondrial permeability transition to lethal injury after exposure of hepatocytes to *t*-butylhydroperoxide. *Biochem. J.* **307**, 99–106.

Palmieri, F. and Klingenberg, M. (1979). Direct methods for measuring metabolite transport and distribution in mitochondria. *Meth. Enzymol*. **55**, 279–301.

Pastorino, J. G., Snyder, J. W., Serroni, A., Hoek, J. B. and Farber, J. L. (1993). Cyclosporin and carnitine prevent the anoxic death of cultured hepatocytes by inhibiting the mitochondrial permeability transition. *J. Biol. Chem*. **268**, 13791–13798.

Pulsford, A. L., Thomas, M. E., Lemaire-Gony, S., Coles, J., Fossato, V. U. and Pipe, R. K. (1995). Studies on the immune system of the goby, *Zosterisessor ophiocephalus*, from the Venice lagoon. *Mar. Pollut. Bull*. **30**, 586–591.

Rigobello, M. P., Toninello, A., Siliprandi, D. and Bindoli, A. (1993). Effect of spermine on mitochondrial glutathione release. *Biochem. Biophys. Res. Commun.* **194**, 1276–1281.

Snyder, J. W., Pastorino, J. G., Attie, A. M. and Farber, J. L. (1992). Protection by cyclosporin A of cultured hepatocytes from the toxic consequences of the loss of mitochondrial energization produced by 1-methyl-4-phenylpyridinium. *Biochem. Pharmac*. **44**, 833–835.

Szabò, I., Bathori, G., Wolff, D., Store, D., Cola, T. and Zoratti, M. (1995). The high-conductance channel of porin-less yeast mitochondria. *Biochim. Biophys. Acta* **1235**, 115–125.

Toninello, A., Miotto, G., Siliprandi, D., Siliprandi, N. and Garlid, K. D. (1988). On the mechanism of spermine transport in liver mitochondria. *J. Biol. Chem*. **263**, 19407–19411.

Toninello, A., Dalla Via, L., Testa, S., Siliprandi, D. and Siliprandi, N. (1990). Transport and action of spermine in rat heart mitochondria. *Cardioscience* **1**, 287–294.

Vianello, A., Macri, F., Braidot, E. and Mokhova, E. N. (1995). Effect of cyclosporin A on energy coupling in pea stem mitochondria. *FEBS Lett.* **371**, 258–260.

Zanzami, N., Susin, S. A., Marchetti, P., Hirsh, T., Gomez–Monterey, I., Castedo, M. and Kroemer, G. (1996). Mitochondrial control of nuclear apoptosis. *J. Exp. Med*. **183**, 1533–1544.

Zoratti, M. and Szabò, I. (1995). The mitochondrial permeability transition. *Biochem. Biophys. Acta* **1241**, 139–176.